

# EUROPEAN ORGANIZATION FOR NUCLEAR RESEARCH

## Proposal to the ISOLDE and Neutron Time-of-Flight Committee

(Following HIE-ISOLDE Letter of Intent I-111)

### First spectroscopy of the the r-process nucleus $^{135}\text{Sn}$

January 10, 2018

Th. Kröll<sup>1</sup>, K. Wimmer<sup>2</sup>, C. Berner<sup>3</sup>, C. Henrich<sup>1</sup>, A.-L. Hartig<sup>1</sup>, G. Fernández Martínez<sup>1</sup>, H.-B. Rhee<sup>1</sup>, I. Homm<sup>1</sup>, C. Sürder<sup>1</sup>, N. Imai<sup>2</sup>, P. Schrock<sup>2</sup>, T. Koiwai<sup>2</sup>, R. Gernhäuser<sup>3</sup>, S. Bishop<sup>3</sup>, A. Jungclaus<sup>4</sup>, J. Cederkäll<sup>5</sup>, P. Golubev<sup>5</sup>, D. Mücher<sup>6</sup>, V. Bildstein<sup>6</sup>, P. Reiter<sup>7</sup>, T. Stora<sup>8</sup>, L. Gaffney<sup>8</sup>, R. Lozeva<sup>9</sup>, N. Pietralla<sup>1</sup>, G. Rainovski<sup>10</sup>, M. Scheck<sup>11</sup>, J. F. Smith<sup>11</sup>, R. Chapman<sup>11</sup>, D. O'Donnell<sup>11</sup>, J. Pakarinen<sup>12,13</sup>, J. Konki<sup>12,13</sup>, J. Ojala<sup>12,13</sup>, R. Raabe<sup>14</sup>, P. Van Duppen<sup>14</sup>, D. Sharp<sup>15</sup>, L. Fraile<sup>16</sup>, J. Benito<sup>16</sup>, and the MINIBALL, T-REX and HIE-ISOLDE collaborations

<sup>1</sup>TU Darmstadt, Germany; <sup>2</sup>Univ. of Tokyo, Japan; <sup>3</sup>TU München, Germany; <sup>4</sup>IEM CSIC, Madrid, Spain; <sup>5</sup>Lunds Univ., Sweden; <sup>6</sup>Univ. of Guelph, Canada; <sup>7</sup>Univ. zu Köln, Germany; <sup>8</sup>CERN, Genève, Switzerland; <sup>9</sup>CSNSM, Orsay, France; <sup>10</sup>Univ. of Sofia, Bulgaria; <sup>11</sup>Univ. of the West of Scotland, Paisley, UK; <sup>12</sup>Univ. of Jyväskylä, Finland; <sup>13</sup>Helsinki Institute of Physics, Finland; <sup>14</sup>KU Leuven, Belgium; <sup>15</sup>Univ. of Manchester, UK; <sup>16</sup>UC Madrid, Spain

**Spokespersons:** Th. Kröll [tkroell@ikp.tu-darmstadt.de], K. Wimmer [wimmer@phys.s.u-tokyo.ac.jp]

**Contact person:** L. Gaffney [liam.gaffney@cern.ch]

**Abstract:** We propose to study states in the isotope  $^{135}\text{Sn}$  populated by a  $^{134}\text{Sn}(d,p)$  one-neutron transfer reaction at 10 MeV/u in inverse kinematics. The experimental set-up will consist of MINIBALL and T-REX. We aim for the identification excited states in this nucleus for the first time. Excitation energies, spin-parity assignments and spectroscopic factors extracted from the data will allow for a stringent test of predictions by state-of-the-art shell model calculations in this region.

**Requested shifts:** [24] shifts, (split into [1] runs over [1] years)

**Installation:** [MINIBALL + T-REX]



# 1 Physics case

The understanding of doubly-magic shell closures is the benchmark for any nuclear theory. On the neutron-rich side of the nuclear chart, the region around  $^{132}\text{Sn}$  is the focus of many efforts in both experimental and theoretical nuclear physics. Additional interest comes from nuclear astrophysics as the r-process<sup>1</sup> approaches  $^{132}\text{Sn}$  from the neutron-rich  $N = 82$  waiting point nuclei, and then proceeds along the  $Z = 50$  isotopic chain towards more neutron-rich nuclei. Masses,  $\beta$  half-lives and  $(n,\gamma)$  rates, all directly linked to the nuclear structure of the involved isotopes, are crucial inputs for the description of the  $A \approx 130$  peak in the solar element abundances [1, 2]. Extrapolation towards heavier Sn isotopes therefore requires a strong anchor point at the doubly-magic  $^{132}\text{Sn}$ . First spectroscopy and neutron spectroscopic factors for  $^{135}\text{Sn}$  will therefore serve as a benchmark for nuclear theory and also give important information on the direct neutron capture process.

Our programme to investigate the nuclear structure in this region at HIE-ISOLDE is sketched in our LoI which has been endorsed by the INTC in 2010 [4]. Based on this, experiments to study the collective properties by Coulomb excitation have been approved, e.g.  $^{134,136}\text{Sn}$  (IS549), or even performed, e.g.  $^{142}\text{Xe}$  (IS548) or  $^{132}\text{Sn}$  (IS551).

Single-particle properties are investigated most directly by nucleon transfer reactions, e.g.  $(d,p)$ , closely related to  $(n,\gamma)$  neutron capture, or  $(t,p)$ . Main observables are the cross sections as well as the energies and the angular distributions of the outgoing protons which allow for the determination of excitation energies, transferred angular momenta and spectroscopic factors. For heavy beams around  $^{132}\text{Sn}$  well-pronounced angular distributions require beam energies of 10 MeV/u as they become available at HIE-ISOLDE in 2018.

Transfer reactions in this region have been pioneered at Oak Ridge National Laboratory some years ago [5]. The reaction  $^{132}\text{Sn}(d,p)$  has been investigated at a beam energy of 4.77 MeV/u detecting only the emitted protons. The ground state and 3 excited states with excitation energies of 854 keV, 1363 keV, and 2005 keV were populated. The energy resolution was just sufficient to resolve these states. Although the angular distributions of the emitted protons were rather smooth at this beam energy, for the two lowest states an assignment of the transferred orbital angular momentum to be  $\Delta\ell = 1$  or 3 was possible. Guided by shell model predictions spin-parity assignments of  $7/2^-$  and  $3/2^-$  for the ground state and the first excited state could be concluded. The tentative  $(1/2^-)$  and  $(5/2^-)$  assignments for the other two excited states as the respective spin-orbit partners are reasonable, but experimentally not confirmed. The  $(9/2^-)$  candidate at 1561 keV was not populated (or only weakly populated and therefore not resolved within the given energy resolution). Theory expects also two further states with  $11/2^-$  and  $13/2^+$ . The  $11/2^-$  state was found at 3570 keV recently populated in one-neutron knockout from  $^{134}\text{Sn}$  and turned out to be neutron-unbound ( $S_n = 2402$  keV) [6]. However, a  $\gamma$ -branch to the ground state of  $^{133}\text{Sn}$  was observed nevertheless. Being a hole-state in the  $N = 82$  neutron core, it is not populated in one-neutron transfer anyway.

Excited states in  $^{133}\text{Sn}$  have been also observed by detecting  $\gamma$ -rays following a  $^{132}\text{Sn}(^9\text{Be}, ^8\text{Be})$  one-neutron reaction [7]. Here, no sensitivity on the transferred orbital angular

---

<sup>1</sup>In 2017, for the first time observations confirmed a binary neutron star merger as an astrophysical site of the r-process with the light curves as indicator for the composition of isotopes produced and their decay [3].

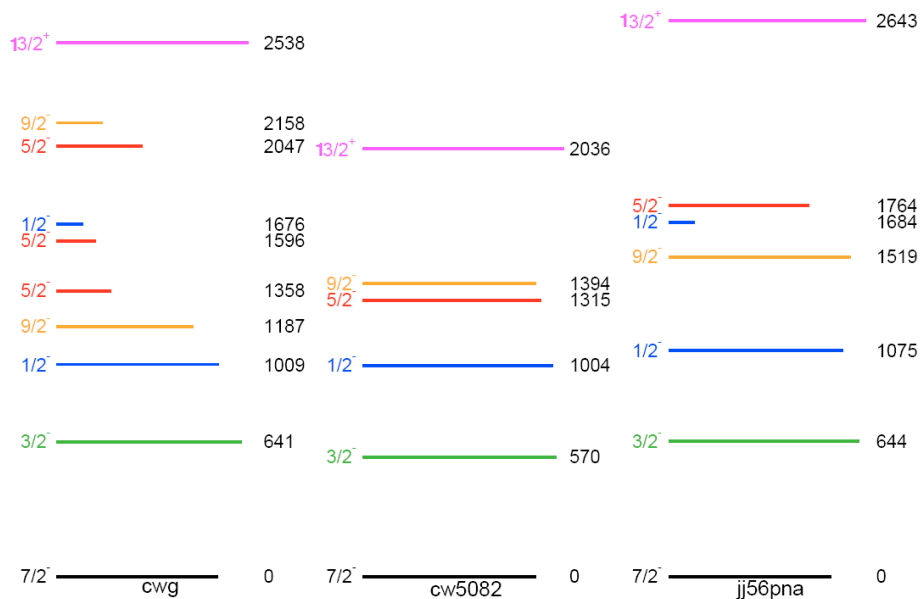


Figure 1: Shell model predictions for  $^{135}\text{Sn}$  with 3 different interactions (see text). The length of the coloured bars for each level corresponds to the spectroscopic factor.

momentum exists. Due to the more complicated wave function, in particular the  $\alpha$  cluster structure of C (and Be, see below), the extracted (relative) spectroscopic factors may be affected. In addition to the states populated in (d,p), with much smaller intensities  $\gamma$ -rays depopulating the  $(9/2^-)$  state as well as a few counts which may indicate the “missing”  $13/2^+$  state to be at 2792 keV have been observed. These complete the expected level scheme for  $^{133}\text{Sn}$ .

The region north-east of  $^{132}\text{Sn}$  has been studied at Oak Ridge as well by  $(^9\text{Be}, ^8\text{Be})$  and  $(^{13}\text{C}, ^{12}\text{C})$  reactions on the more abundant beams of  $^{134}\text{Te}$  and (stable)  $^{136}\text{Xe}$  at 4.2 MeV/u and 4.1 MeV/u, respectively [8]. The higher statistics allowed not only for particle- $\gamma$ - $\gamma$  coincidences but also for particle- $\gamma$  angular correlations giving further confidence in the spin-parity assignments. Noteworthy, the properties of the 3 excited states populated in  $^{137}\text{Xe}$  only partially agree with states among the 18 excited states from  $^{136}\text{Xe}(d,p)$  in inverse kinematics at 10 MeV/u performed at Argonne National Laboratory [9].

In conclusion, transfer reactions, in particular (d,p), are a valuable tool to populate states in exotic nuclei in this region<sup>2</sup> and the combination of a particle detector with large angular coverage to detect the protons with an efficient HPGe array to detect  $\gamma$ -rays in coincidence is the most powerful instrumentation.

**Experimentally, no excited state in  $^{135}\text{Sn}$  is known so far.** Fig. 1 shows the shell model predictions obtained with 3 different interactions concerning the neutron sector [10, 11, 12] which are used in this region of the nuclear chart<sup>3</sup>. For clarity, only states with a spectroscopic factor larger than 0.1 are plotted. The excitation energies of the first two excited states don’t differ much, whereas for the next states, i.e. the  $5/2^-$  and the the

<sup>2</sup>For completeness: spectroscopic information for even Sn isotopes beyond  $^{132}\text{Sn}$  is known from Coulomb excitation of  $^{134}\text{Sn}$  [19] and isomer decays in  $^{134,136,138}\text{Sn}$  [20, 25].

<sup>3</sup>Other calculations with similar predictions can be found in Refs. [23, 13].

$9/2^-$ , even the ordering is predicted differently. Only one of the interaction predicts the  $13/2^+$  state to be bound ( $S_n(^{135}\text{Sn}) = 2271$  keV). However, also if unbound its  $\gamma$ -decay may be observed (as for the  $11/2^-$  and  $13/2^+$  states in  $^{133}\text{Sn}$ ). The length of the coloured bars shows the respective spectroscopic factors. Mostly, the values are well above 0.5 indicating that a strong population of these states can be expected. The fragmentation of the  $5/2^-$  strength predicted by one of the calculations is a notable exception.

Various approaches have been used to generate shell-model interactions capable of predicting the behavior of neutron-rich nuclei beyond  $N = 82$ . Calculations with empirical interactions even predict a new shell closure at  $N = 90$  when the  $\nu f_{7/2}$  orbital is filled, e.g. Ref. [22]. Such an effect is not found in calculations with realistic interactions based on nucleon-nucleon potentials, e.g. Refs. [23, 21]. Including three-body forces, the new shell closure occurs with realistic interactions too [24].

Shell model calculations need, apart from a set of interaction matrix elements, also spectroscopic information from the nuclei neighbouring the doubly-magic cores. E.g. the region north-east of  $^{132}\text{Sn}$  requires the single-particle energies of states in  $^{133}\text{Sn}$  and  $^{133}\text{Sb}$  as input. The validity of the calculations can be tested only with nuclei further away from the core and therefore, keeping the magic closure at  $Z = 50$ , the spectroscopy of  $^{135}\text{Sn}$  is the straightforward challenge for the predictive power towards neutron-rich isotopes.

The structure of the Sn isotopes is particularly important to test the neutron-neutron part of shell-model interactions as proton-proton and proton-neutron terms do not contribute at low energies and, therefore, low-lying states have a pure neutronic character. The results of the proposed experiment will aid the understanding of the evolution of neutron-neutron two-body matrix elements in nuclei with large neutron excesses.

## 2 Experimental method and set-up

We will apply the method of particle spectroscopy in combination with  $\gamma$ -ray spectroscopy following a one-neutron (d,p) transfer reaction. The set-up will consist of MINIBALL [29] and T-REX [30]. This set-up with T-REX in slightly differing configurations adapted to the particular experiment has been successfully used to study transfer reactions at REX-ISOLDE, e.g. Refs. [14, 15, 16, 17, 18].

Fig. 2 shows the calculated angular distributions of the protons following the  $^{134}\text{Sn}(d,p)$  ( $Q_0 = 45.2$  keV) reaction in inverse kinematics at 10 MeV/u. The optical model parameters from Ref. [32] have been used. The main part of the transfer cross section is in the backward hemisphere in the laboratory system (Fig. 2, right). The transferred orbital angular momenta  $\Delta\ell = 1$  and 3 are clearly distinguishable. Even for the large  $\Delta\ell = 5$  and 6, a different slope above  $100^\circ$  in the lab system is easily seen (Fig. 2, right).

The higher beam energy at HIE-ISOLDE compared to our previous experiments at REX-ISOLDE results in larger energies of the detected particles. In forward direction, most elastically scattered deuterons, needed to adapt the optical model parameters and to determine the normalisation luminosity, as well as protons from the reaction are not stopped in the present T-REX configuration. Our simulations have shown that measuring twice an energy loss is sufficient to determine the energy and identify the particle. As in previous experiments, a thin mylar foil will be placed in front of the forward detectors to

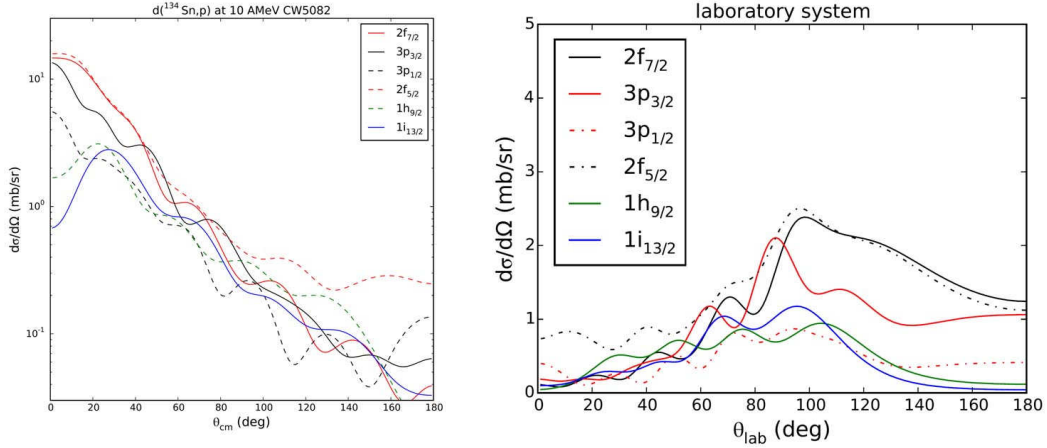


Figure 2: Angular distributions of protons following the  $^{134}\text{Sn}(d,p)$  reaction at 10 MeV/u. Excitation energies and spectroscopic factors are calculated with the cw5082 interaction.

stop elastically scattered  $^{12}\text{C}$  ions from the target.

The weakest point of T-REX in its present implementation are the backward barrel detectors ( $100^\circ < \vartheta_{\text{Lab}} < 150^\circ$ ) because of their low segmentation and large sensitivity to noise, pickup and  $\delta$ -electrons. For the proposed experiment this angular region is essential (see Fig. 2, right). We will replace them by segmented Si strip detectors. The detectors are available from another experiment [28] and are compatible once the internal holding structure of T-REX is appropriately modified. The improvement can be seen in the results from a full GEANT simulation in Fig. 3 with a 1 mg/cm<sup>2</sup> target<sup>4</sup>. Some levels populated in the reaction are clearly resolved, even without the help of coincident  $\gamma$ -rays. The protons from the  $^{134}\text{Sb}(d,p)$  reaction will be detected too, at higher energies because of the larger  $Q_0 = 1516.5$  keV.

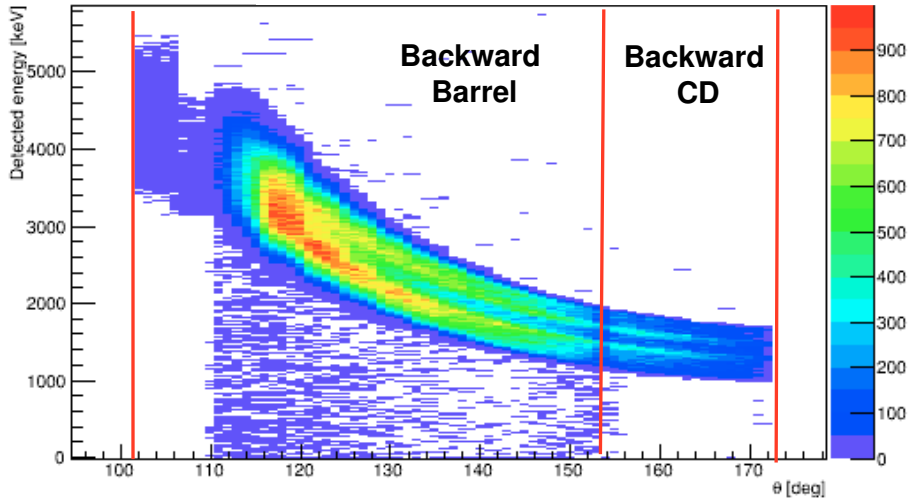


Figure 3: Simulated proton energy versus scattering angle in the laboratory system.

From the experience with  $^{132}\text{Sn}$  (IS551, 2016) [26], we expect only Sb as contamination. As the Sn/Sb production ratio at  $A = 134$  is less favourable compared to  $A = 132$

<sup>4</sup>For clarity, only the first 4 states as predicted with the cw5082 interaction have been included.

(measured value for beam on target was 2.18), we expect a rather large contamination. In addition, the isotope  $^{134}\text{Sn}$  ( $T_{1/2} = 1.06$  s [27]) will decay to a small amount during trapping and breeding to  $^{134}\text{Sb}$ , about 10 %. Similar values have been measured for  $^{142}\text{Xe}$  ( $T_{1/2} = 1.23$  s) during the IS548 campaign in 2016.

The separation of isobars of two neighbouring elements with  $A = 134$  is on the edge of the capability of the IC-Si telescope in the beamdump. The beam composition will be determined from the characteristic  $\gamma$ -rays from the decay of the Sn and Sb isotopes too. Occasionally, the beam may be stopped at the target position within MINIBALL.

### 3 Rate estimate and beam time request

The Sn isotope is produced with a standard  $\text{UC}_x/\text{graphite}$  target irradiated with the proton beam from the PS Booster. In order to eliminate the Cs contamination, as used in experiment IS551 (2016), we will extract  $\text{SnS}^+$  molecules which will be cracked afterwards in the EBIS [33]. Natural sulphur contains the isotopes  $^{32,33,34,36}\text{S}$  (94%, 0.75%, 4.2%, 0.02%). To produce  $^{134}\text{Sn}$ , a  $A = 166$  beam would contain  $^{134}\text{Sn}^{32}\text{S}^+$  but also a strong contamination from the more abundant Sn isotope, hence  $^{132}\text{Sn}^{34}\text{S}^+$ . Therefore, we will use isotopically enriched  $^{34}\text{S}$  and produce a very clean  $A = 168$  beam containing only  $^{134}\text{Sn}^{34}\text{S}^+$  molecules [33]. Newer developments of the ISOLDE target group with the VADIS ion source enable a yield of about  $10^5/\mu\text{C}$  for  $^{134}\text{Sn}$  [34].

The isotope  $^{134}\text{Sn}$  decays subsequently to the stable Xe isobar. The decay products involved with longest half-lives are  $^{134}\text{I}$  (52 min) and  $^{134}\text{Te}$  (41.8 min). Therefore, activation by long-lived decay products is no issue for the experiment and radiation protection.

Assuming a proton current of  $2 \mu\text{A}$  and, conservatively, an efficiency of HIE-ISOLDE of 5% the expected beam intensity will be  $10^4/\text{s}$ . We require the slow extraction from the EBIS to reduce the instantaneous particle rate.

Assuming a standard deuterated PE target of  $1 \text{ mg}/\text{cm}^2$  thickness the count rate per 1 mb of cross section and  $10^4/\text{s}$  incoming particles is 650/day. The integrated cross section for the region covered by the backward barrel of T-REX is about 2-8 mb (taking into account a reduction of the spectroscopic factors by a factor of 0.7). Dividing the data set into 6-10 angular bins results in about 300 counts per bin and day. In 8 days of beam time, a statistical error per bin of 2% can be achieved.

However, in most cases the coincident  $\gamma$ -rays are needed to separate the states and to determine, in particular in  $^{135}\text{Sn}$  the exact excitation energies. New  $\gamma$ -rays not belonging to  $^{135}\text{Sb}$ , whose level scheme is well known from decay spectroscopy at ISOLDE [35, 36], in coincidence with protons having the correct kinematics unambiguously assign these to  $^{135}\text{Sn}$ . The rates for proton- $\gamma$  coincidences will be, depending on the energy of the  $\gamma$ -ray, by a factor of about 10-30 smaller. Hence, the statistical error per bin will be around 10% (assuming only one decay branch), which is sufficient to distinguish the different orbital angular momentum transfers  $\Delta\ell$  (see Fig. 2, right). In case, if a weak transition is observed or if  $\gamma$ - $\gamma$ -coincidences turn out to be helpful from the online analysis, a thicker target can be used for a limited time too.

**Summary of requested shifts: we request 8 days (24 shifts) of  $^{134}\text{Sn}$  beam.**

## References

- [1] R. Surman et al., Phys. Rev. C 79, 045809 (2009).
- [2] G. Lorusso et al., Phys. Rev. Lett. 114, 192501 (2015).
- [3] I. Arcavi et al., Nature 551, 64 (2017); M. R. Drout et al., Science 10.1126/science.aag0049 (2017); many more
- [4] Th. Kröll et al., CERN-INTC-2010-045 / INTC-I-111.
- [5] K. L. Jones et al., Nature 465, 454 (2010).
- [6] V. Vacquero et al., Phys. Rev. Lett. 118, 202502 (2017).
- [7] J. M. Allmond et al., Phys. Rev. Lett. 112, 172701 (2014).
- [8] J. M. Allmond et al., Phys. Rev. C 86, 031307(R) (2012).
- [9] B. P. Kay et al., Phys. Rev. C 84, 024325 (2011).
- [10] W.-T. Chou and E. K. Warburton, Phys. Rev. C 45, 1720 (1992).
- [11] B. A. Brown et al., Phys. Rev. C 71, 044317 (2005).
- [12] B. A. Brown (2012).
- [13] L. Y. Jia et al., Phys. Rev. C 76, 054305 (2007).
- [14] K. Wimmer et al., Phys. Rev. Lett. 105, 252501 (2010).
- [15] J. Johansen et al., Phys. Rev. C 88, 044619 (2013).
- [16] J. Diriken et al., Phys. Lett. B 736, 533 (2014).
- [17] R. Orlandi et al., Phys. Lett. B 740, 238 (2015).
- [18] K. Nowak et al., Phys. Rev. C 93, 044335 (2016).
- [19] R. L. Varner et al., Eur. Phys. J. A 25, s01, 391 (2005).
- [20] A. Korgul et al., Eur. Phys. J. A 7, 167 (2000).
- [21] A. Covello et al., J. Phys.: Conf. Ser. 267, 012019 (2011).
- [22] S. Sarkar and M. Saha Sarkar, Phys. Rev. C 78, 024308 (2008).
- [23] M. P. Kartamyshev et al., Phys. Rev. C 76, 024313 (2007).
- [24] S. Sarkar and M. Saha Sarkar, J. Phys.: Conf. Ser. 267, 012040 (2011).
- [25] G. S. Simpson et al., Phys. Rev. Lett. 113, 132502 (2014).

- [26] D. Rosiak et al., ISOLDE workshop (2017).
- [27] <http://www.nndc.bnl.gov>
- [28] P. Golubev et al., Nucl. Instr. Meth. A 723, 55 (2013).
- [29] N. Warr et al., Eur. Phys. J. A 49, 40 (2013).
- [30] V. Bildstein et al., Eur. Phys. J. A 48, 85 (2012).
- [31] Th. Kröll, G. Simpson et al., CERN-INTC-2012-042 / INTC-P-343.
- [32] C. Perey and F. Perey, At. Data Nucl. Data Tables 17, 1 (1976).
- [33] U. Koester et al., Nucl. Instr. Meth. B 266, 4229 (2008).
- [34] T. Stora, private communication.
- [35] J. Shergur et al., Phys. Rev. C 72, 024305 (2005).
- [36] H. Mach et al., Acta Phys. Pol. B 38, 1213 (2007).



# Appendix

## DESCRIPTION OF THE PROPOSED EXPERIMENT

The experimental setup comprises: (*MINIBALL + T-REX*)

Part of the	Availability	Design and manufacturing
(if relevant, name fixed ISOLDE installation: [MINIBALL + T-REX])	<input checked="" type="checkbox"/> Existing	<input checked="" type="checkbox"/> To be used without any modification
[MINIBALL]	<input checked="" type="checkbox"/> Existing	<input checked="" type="checkbox"/> To be used without any modification <input type="checkbox"/> To be modified
	<input type="checkbox"/> New	<input type="checkbox"/> Standard equipment supplied by a manufacturer <input type="checkbox"/> CERN/collaboration responsible for the design and/or manufacturing
[CD]	<input checked="" type="checkbox"/> Existing	<input checked="" type="checkbox"/> To be used without any modification <input type="checkbox"/> To be modified
	<input type="checkbox"/> New	<input type="checkbox"/> Standard equipment supplied by a manufacturer <input type="checkbox"/> CERN/collaboration responsible for the design and/or manufacturing
[insert lines if needed]		

HAZARDS GENERATED BY THE EXPERIMENT (if using fixed installation:) Hazards named in the document relevant for the fixed [MINIBALL + T-REX] installation.

Additional hazards:

Hazards	[Part 1 of experiment/ equipment]	[Part 2 of experiment/ equipment]	[Part 3 of experiment/ equipment]
<b>Thermodynamic and fluidic</b>			
Pressure	[pressure][Bar], [volume][l]		
Vacuum			
Temperature	[temperature] [K]		
Heat transfer			
Thermal properties of materials			
Cryogenic fluid	[fluid], [pressure][Bar], [volume][l]		
<b>Electrical and electromagnetic</b>			
Electricity	[voltage] [V], [current][A]		
Static electricity			
Magnetic field	[magnetic field] [T]		
Batteries	<input type="checkbox"/>		

Capacitors	<input type="checkbox"/>		
<b>Ionizing radiation</b>			
Target material [material]			
Beam particle type (e, p, ions, etc)			
Beam intensity			
Beam energy			
Cooling liquids	[liquid]		
Gases	[gas]		
Calibration sources:	<input type="checkbox"/>		
• Open source	<input type="checkbox"/>		
• Sealed source	<input type="checkbox"/> [ISO standard]		
• Isotope			
• Activity			
Use of activated material:			
• Description	<input type="checkbox"/>		
• Dose rate on contact and in 10 cm distance	[dose][mSV]		
• Isotope			
• Activity			
<b>Non-ionizing radiation</b>			
Laser			
UV light			
Microwaves (300MHz-30 GHz)			
Radiofrequency (1-300 MHz)			
<b>Chemical</b>			
Toxic	[chemical agent], [quantity]		
Harmful	[chem. agent], [quant.]		
CMR (carcinogens, mutagens and substances toxic to reproduction)	[chem. agent], [quant.]		
Corrosive	[chem. agent], [quant.]		
Irritant	[chem. agent], [quant.]		
Flammable	[chem. agent], [quant.]		
Oxidizing	[chem. agent], [quant.]		
Explosiveness	[chem. agent], [quant.]		
Asphyxiant	[chem. agent], [quant.]		
Dangerous for the environment	[chem. agent], [quant.]		
<b>Mechanical</b>			

Physical impact or mechanical energy (moving parts)	[location]		
Mechanical properties (Sharp, rough, slippery)	[location]		
Vibration	[location]		
Vehicles and Means of Transport	[location]		
<b>Noise</b>			
Frequency	[frequency],[Hz]		
Intensity			
<b>Physical</b>			
Confined spaces	[location]		
High workplaces	[location]		
Access to high workplaces	[location]		
Obstructions in passageways	[location]		
Manual handling	[location]		
Poor ergonomics	[location]		

Hazard identification:

Average electrical power requirements (excluding fixed ISOLDE-installation mentioned above): [make a rough estimate of the total power consumption of the additional equipment used in the experiment]